

A generative model of white matter axonal orientations near the cortex

Michiel Cottaar¹, Saad Jbabdi¹, Matthew F Glasser², Krikor Dikranian², David C van Essen², Timothy E Behrens¹, and Stamatis N Sotiropoulos¹
¹FMRIB Centre, University of Oxford, Oxford, United Kingdom, ²Washington University School of Medicine, Saint Louis, Missouri, United States

Target audience: This work impacts tractography close to the cortical surface and so should interest researchers studying cortical structural connectivity as well as those modelling low-level diffusion MRI data.

Purpose: Diffusion-weighted MRI data is sensitive to the diffusion of water on the size scale of individual axons, which allows the orientation of these axons to be measured. However, the data is acquired at a much coarser resolution of about $(1\text{-}2\text{ mm})^3$ in living humans. This coarse resolution can hide small-scale structure, especially close to the cortical surface where axons often bend sharply towards the grey matter (GM)/ white matter (WM) boundary [1]. Classical tractography algorithms [2, 3] follow the peak of the fibre orientation distribution function (ODF) derived from the diffusion MRI signal, which causes the streamlines to ignore these sharp, sub-voxel bends and continue to the tip of the cortical gyri [4]. However, the diffusion MRI signal does contain information about these bends through the dispersion of the fibre ODF [5, 6, 7]. Here we propose a simple model of the axonal orientations within an entire gyrus with few enough parameters that it can be fitted to the low-resolution diffusion MRI data, but can still accurately describe the axonal orientations seen in a much higher-resolution histology dataset ($\sim\mu\text{m}^2$).

Methods: Here we describe the gyral axonal orientation model as well as the histology data used to validate this model

Model: The axonal orientation at point x in the WM is modelled to be parallel to

$\int ds \left(\hat{\theta}(s) + \frac{b(s)}{d(s,x)} \hat{r}(s) \right) d(s,x)^{-1}$, where we integrate over the full GM/WM boundary within a gyrus parameterized by s . $d(s,x)$ is the Euclidean distance between point x and the GM/WM boundary at s , $\hat{r}(s)$ is a unit vector oriented perpendicular to the GM/WM boundary at s , and $\hat{\theta}(s)$ is a unit vector oriented parallel to the GM/WM boundary, which is chosen to point away from the gyral crown. Finally the bending parameter $b(s)$ is the only free parameter, which can either be constant (single-parameter model) or vary across the GM/WM boundary. In this model, fibre orientations are perpendicular to the GM/WM boundary close to this boundary (for $d(s,x) < b(s)$) and become parallel to the GM/WM boundary in the deeper white matter (for $d(s,x) > b(s)$). So a small bending parameter $b(s)$ implies that only the axons closest to the GM/WM boundary bend towards the surface, while a larger range of axons bend towards the surface, where the bending parameter $b(s)$ is large.

Although we apply it to 2-dimensional histology data here, the model can be trivially extended to 3 dimensions by allowing $b(s)$ to vary across the two-dimensional GM/WM boundary and integrating over this full surface.

Histology data: To validate the accuracy of this model at small spatial scales we use an image of a myelin-stained gyral slice of a postnatal day 6 macaque brain (Figure 1) at a resolution of about $(9\text{ }\mu\text{m})^2$ [4, 5]. The orientation of the axons was estimated through structure tensor analysis [5, 8]. At every pixel the axons are assumed to be perpendicular to the direction of the maximum intensity gradient. These local orientations are smoothed by a Gaussian filter with a sigma of 20 pixels for stability. The resulting color-coded orientations are plotted in Figure 1 (up-down in green and left-right in red). The GM/WM boundary needed for the model was manually drawn on this occasion. We fit the model to these observed axonal orientations by minimizing the quadratic sum of pixel-wise angular deviations between the observed and predicted axonal orientations in the WM.

Results: Figure 2 shows the best-fit single-parameter model for which we find a bending parameter $b(s) \approx 0.15\text{ mm}$. Already this model accurately fits the WM axonal orientation with an average angular error of only 4° . We can learn more about the axonal connectivity to the GM/WM boundary by allowing the bending parameter to vary. Figure 3 shows the best-fit five-parameter model, where we split the GM/WM boundary into three parts with different bending parameters (3 variables) and variable boundaries (2 variables). The bending parameter $b(s)$ is found to be low close to the base of the gyrus or on the right gyral wall (0.02 and 0.12 mm respectively), while the axons are found to bend to the GM/WM boundary over a larger range at left gyral wall ($b(s) \approx 0.3\text{ mm}$). This five-parameter model has an average angular error of only 2.5° across the WM.

Discussion: Here we developed a simple model that can reproduce within 4° the axonal orientations from histological data through an entire gyral slice with only a single free parameter, which we refer to as the bending parameter $b(s)$. A high bending parameter implies the axons bend towards the surface over a large WM area, which should correspond to a high structural connectivity. Indeed we find relatively many axons penetrating the grey matter at the left gyral wall (Figure 1), where the bending parameter measured in the white matter is the largest (Figure 3). The bending parameter is small (up to 0.3 mm) compared to the typical resolutions obtained in diffusion MRI data, which confirms that the axons bend to the cortical surface at a sub-voxel resolution and thus can only be detected in diffusion MRI through the dispersion of the fibre ODF [5, 6, 7]. Low-parameter models of axonal orientation such as the one presented here are crucial to correctly reproduce the axonal distribution underlying this dispersion and hence to derive accurate structural connectivity to the cortical surface.

References: 1. Jbabdi & Johansen-Berg, Brain Connectivity 1: 169-83, 2011. 2. Basser et al, 2000, Magn Reson Med 44: 625. 3. Behrens et al, 2003, Magn Reson Med 50:1077. 4. Van Essen et al, Diffusion MRI (2nd Edition), Elsevier, 337-358, 2013. 5. Sotiropoulos et al, ISMRM, 835, 2013. 6. Sotiropoulos et al, Neuroimage 60:1412-1425, 2012. 7. Zhang et al, Neuroimage 61:1000-1016, 2012. 8. Budde et al, Neuroimage 63:1-10, 2012.

Acknowledgment: We would like to acknowledge funding from the UK Wellcome Trust (098369/Z/12/Z) and EPSRC (EP/L023067/1).

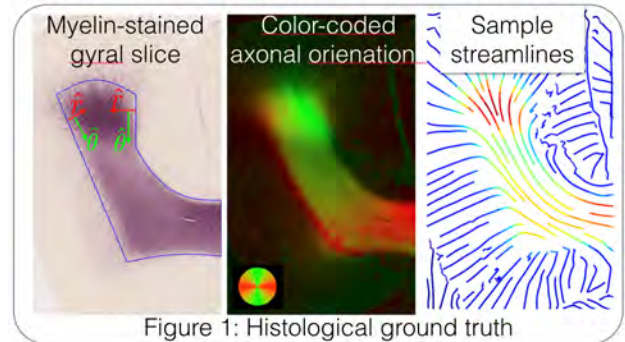


Figure 1: Histological ground truth

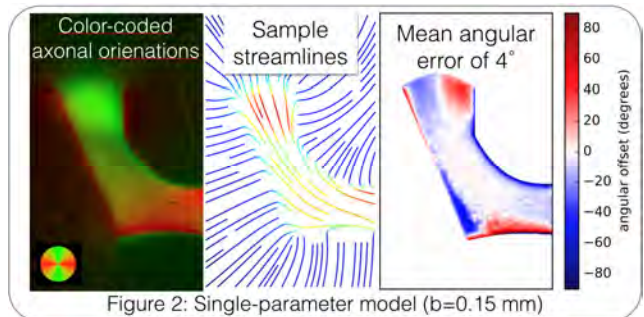


Figure 2: Single-parameter model ($b=0.15\text{ mm}$)

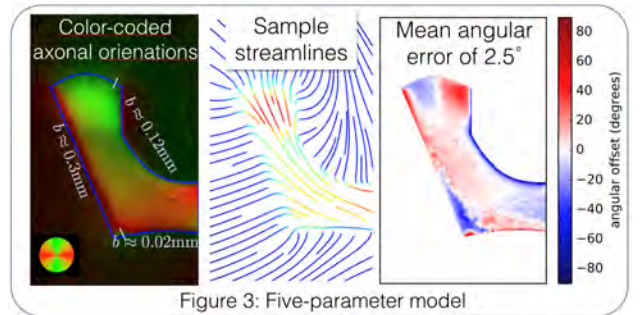


Figure 3: Five-parameter model